論文 86-23-4-22

A Analysis of Phase and Time Domain Characteristics of Elliptic Filters

(楕圓필터의 位相 및 時間領域 特性 分析)

李鍾寅*, 金東龍*, 申建淳**

(Chong In Lee, Dong Yong Kim and Gun Soon Shin)

要 約

본 논문에서는 일립틱함수 필터의 저지대역(stopband) 주파수 ω_s와 통과대역 리플(passband ripple) A_p의 변화에 따르는 영점-극점 추이(pole-zero shifting)를 연구하였다.

그리고, 이필터의 위상특성, 군지연(group-delay)특성, 단위스탭과 임펄스 응답특성을 조사분석 하였다. 그 결과 ω_s를 증가시키므로써 통과대역에서의 위상선형특성이 증진되는 것을 고찰하였고 그 결과가 체비셰프 함수 필터의 위상선형 특성에 접근함을 알 수 있었다.

Abstract

In this paper, we have investigated pole-zero shifting due to variable stopband frequency ω_S and passband ripple A_p of elliptic function filters. Also, we have studied the phase, group-delay, unit step response and impulse response of elliptic filters. We show that in the passband the phase linearity improves as ω_S increases, and eventually it approaches that of a chebyshev function filter.

I. Introduction

Filter networks are of great importance, not only in communication engineering, but also in all fields of electrical measurement and equipment engineering.

The Elliptic characteristic has a ripple in both the passband and stopband. The ripple in the stopband is produced by *jw* axis poles. This is the reason for the large attenuation slope at the band edge. Due to this property, the Elliptic magnitude characteristic is one of the most useful in the design and synthesis of filter networks.

Filter behavior in the frequency domain is important in communication technology. However, the behavior of filters in time domain and the consideration of their response to input signals given as time function is just as important. Time domain characteristics of the input and output signals of a system are measured through the output signal distortion. Any realizable system has an output that is distorted from the input in various ways. Impulse response and step response are two outputs which are often used to measure the distortion.

The purpose of this paper is to discuss

*正會員, 全北大學校 電氣工學科
(Dept. of Electrical. Eng., Chonbuk Nat'l Univ.)
**正會員, 金烏工大 電子工學科
(Kum Oh Institute of Technology)
接受日字: 1986年 1月 10日

briefly the phase, group-delay, unit step response and impulse response of Elliptic filters.

II. Pole-Zero Shifting of an Elliptic Function

For convenience, the elliptic function may be written as [1,2,3]

$$H(s) = K \prod_{i=1}^{n/2} \frac{S^2 + c_i}{S^2 + a_i S + b_i} \quad \text{n: even} \qquad (1a)$$

$$H(s) = \frac{K}{S+\sigma_0} \prod_{i=1}^{(n-1)/2} \frac{S^2 + c_i}{S^2 + a_i S + bi} \quad \text{n: odd} \qquad (1b)$$

The typical pole-zero locations and the magnitude characteristics are illustrated in Fig. 1 for n = 6 and n = 7, respectively [3,4].

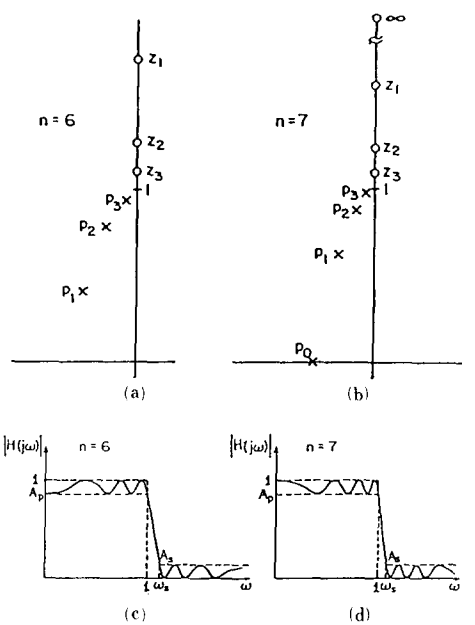

Fig. 1. (a) Pole-zero plot of typical elliptic function of n = 6,
(b) Pole–zero plot of typical elliptic function of n = 7,
(c) The magnitude characteristic for n = 6,
(b) The magnitude characteristic for n = 7.

As shown in Fig. 1(c) and (d), the stopband frequency ω_s is the frequency where stopband begins. This parameter is used in this paper instead of a modular angle θ so that we may assign adequate values for

$$\theta = \sin^{-1} \frac{1}{\omega_s} \qquad (2)$$

Furthermore the passband ripple A_p (dB)=−20 log A_p will be specified instead of the reflection coefficient ρ.

$$A_p(\text{dB}) = -10 \log \left[1 - \left(\frac{\rho}{100}\right)^2 \right] \qquad (3)$$

There are tables in the reference [4] from which we can find the order of the filter function for given passband ripples A_p(dB), stopband ateenuation A_s (dB) and the stopband frequency ω_s. For a given passband ripple A_p and the order n, the stopband attenuation A_s becomes larger as ω_s assumes larger values. In this paper we assign ω_s = 1.1, 2.0 to observe the way poles and zeros shift in the complex s-plane. As shown in Fig. 2 the pole- Q decreases as ω_s increases and the pole location converges to Chebyshev point C. On the other hand, as A_p increases poles shift toward the *jw*-axis inducing higher Q's. The pole on the negative real axis shifts nearer the origin and transmission zeros on the *jw*-axis on the other hand move further away from the origin. Their locations are independent of A_p values.

III. Phase and Group-Delay

Since all the zeros are greater than unity (cutoff frequency) and are located on the *jw*-axis, they do not affect the passband phase characteristic of the elliptic filters [4,7], Using (1) the phase is computed as follows.

$$\phi(\omega) = -\sum_{i=1}^{n/2} \tan^{-1} \frac{a_i \omega}{b_i - \omega^2} + \Sigma 180° \mid \omega \geqslant \sqrt{c_i}$$

n: even (4a)

$$\phi(\omega) = -\tan^{-1} \frac{\omega}{\sigma_0} - \sum_{i=1}^{(n-1)/2} \frac{a_i \omega}{b_i - \omega^2} + \Sigma 180° \mid \omega \geqslant \sqrt{c_i}$$

n: odd (4b)

At every frequency greater than $j\sqrt{C_i}$ in (1), the phase will be reduced by 180° due to the

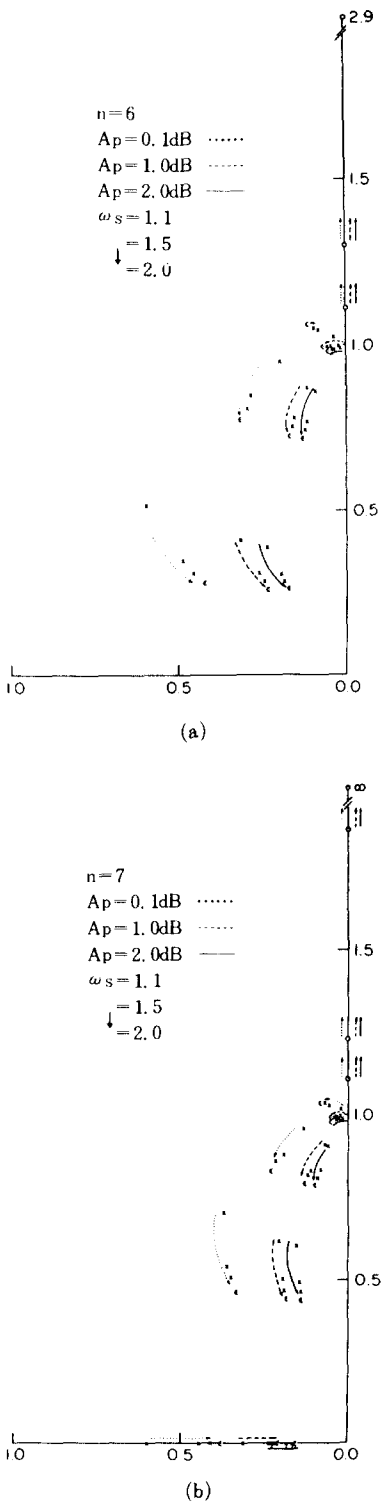

Fig. 2. Pole-zero shifting due to variable stop-band frequency ω_s and passband riple Ap: (a) n = 6, (b) n = 7.

numerator of (1).

In the passband the phase linearity improves as ω_s increases and eventually it approaches that of Chebysheve filter. As seen in fig. 2 phase linearity improves with increasing ω_s due to lower Q values. Smaller A_p improves phase linearity for similar resons. In Fig. 3 the phase characteristics are drawn for ω_s = 1.1, 2.0, and for passband ripples of A_p =1.0.

For even order function, passive ladder realization does not exist. The need for trans-

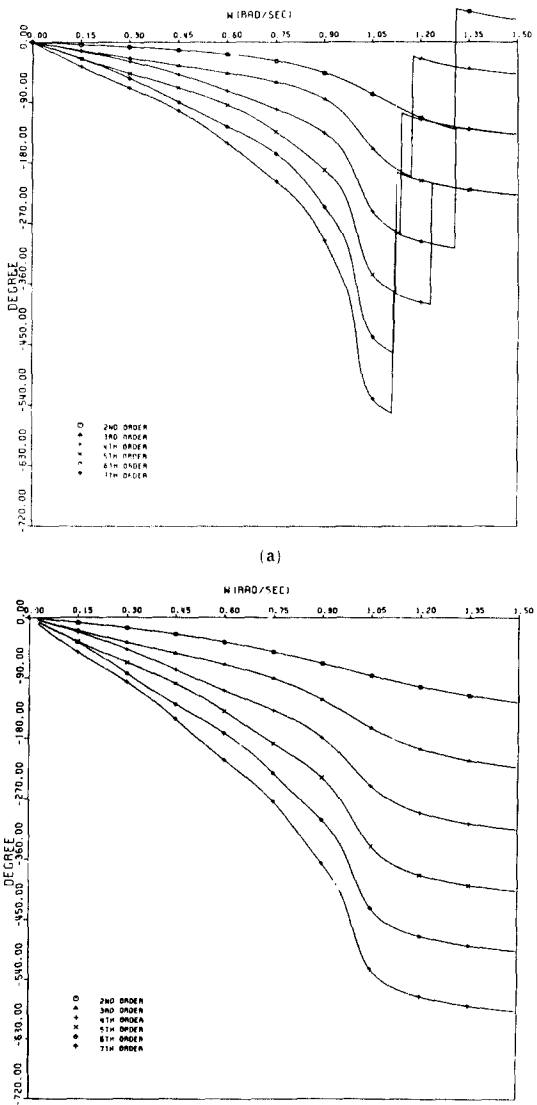

Fig. 3. Phase characteristics for Ap = 1.0 : (a) ω_s = 1.1, (b) ω_s = 2.0.

formers may be eliminated by modifying the function so that the function vanishes at s = ∞. The order of the numerator is (n−2) while that of the denominator is n. There are two kinds of possible transformations: One having a dent at s=0 and the other having no attenuation at s=0. The former is classified as Case B, and the latter as Case C. For comparison the original even function is called Case A. These three Cases are shown in Fig.4 for n=4 including the locations of the highest Q pole. Case A is the closest to the jw-axis, Case B and C follow in that order. Phase characteristics of Cases A, B, and C are plotted in Fig. 5 for n=4 and n=6.

Phases of Case A and Case B are almost identical and the linearity improves in Case C due to lower Q value. Group-delay characteristics are obtained by differentiating (4) with respect to ω. They are plotted on Fig.

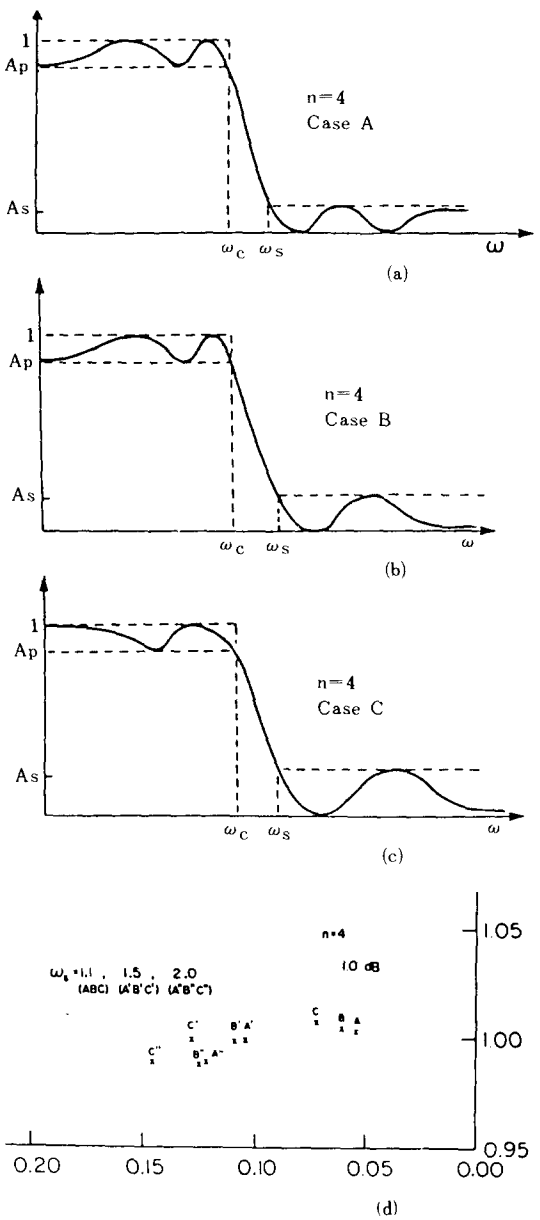

Fig. 4. Typical magnitude characteristics of: (a) Case A, (b) Case B, (c) Case C and (d) high-Q pole shifting.

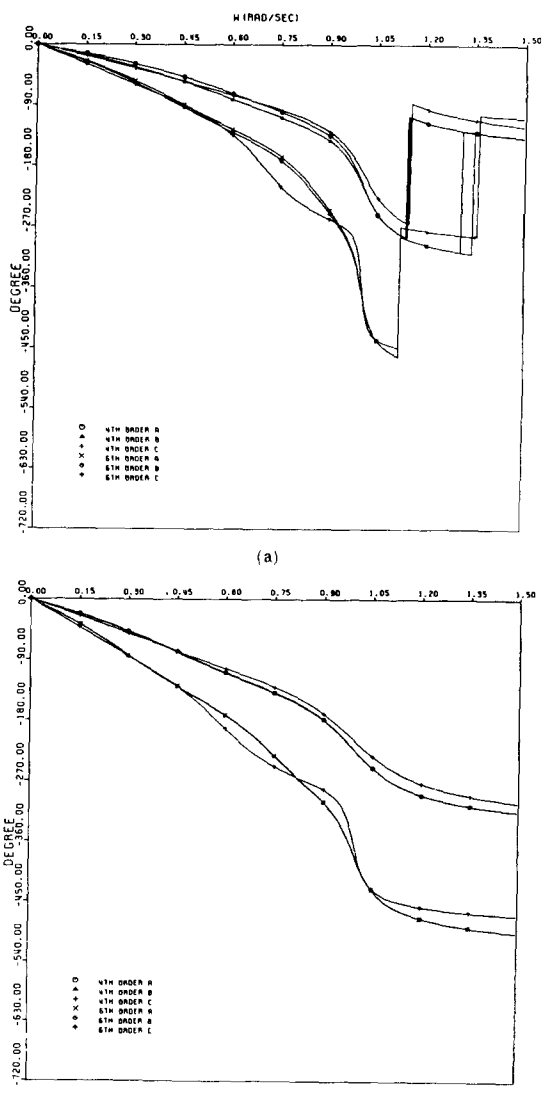

Fig. 5. Phase comparison of Cases A, B, C for Ap = 1.0 : (a) ω_s = 1.1, (b) ω_s = 2.0.

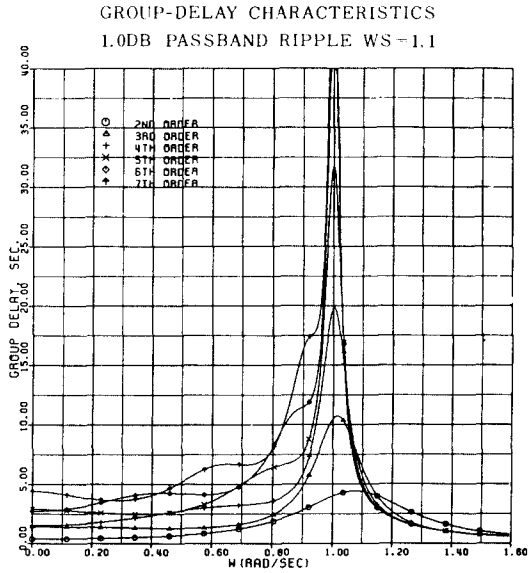

(a)

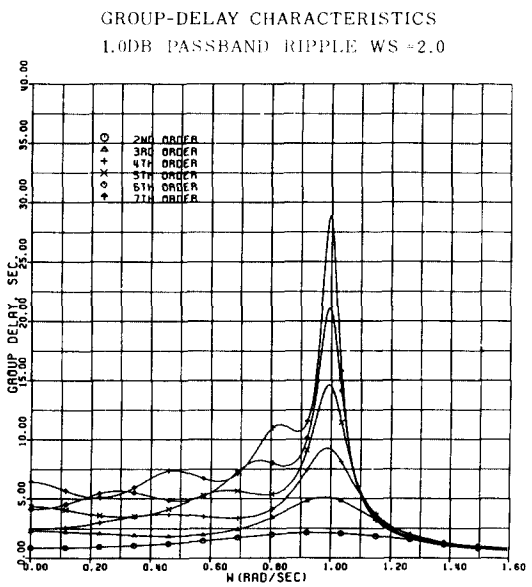

(b)

Fig. 6. Group-delay for Ap = 1.0 : (a) $\omega_s = 1.1$, (b) $\omega_s = 2.0$.

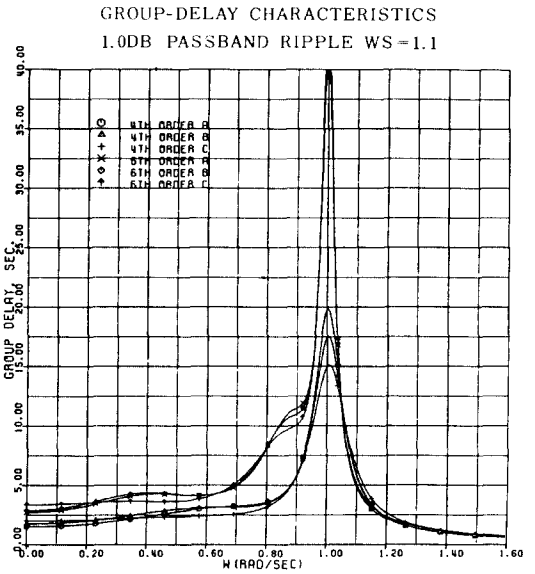

(a)

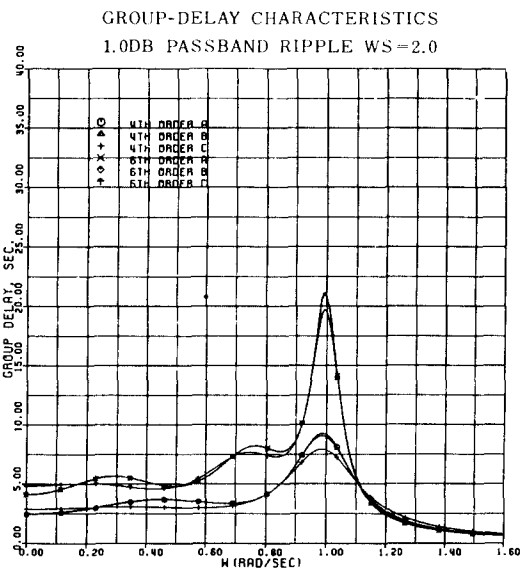

(b)

Fig. 7. Group-delay comparison: (a) $\omega_s = 1.1$, (b) $\omega_s = 2.0$.

6 and Fig. 7. As confirmed by the phase curves, the flatness of the group-delay improves for larger ω_s, smaller A_p (dB) and lower order n. Case A, B, and C are compared in Fig. 7 for n=4 and n=6.

IV. Unit Step Responses

Due to the transmission zeros on the finite point on the *jw*-axis and poles of relatively high Q, the time domain behaviors of the elliptic filters are considerably different from those of all pole function filters such as Butterworth or Chebyshev.

The unit step response can be expressed as follows.

$$a(t)=1+\sum_{i=1}^{n/2}A_i e^{-\frac{a_i}{2}t}\cos(\omega_i t+\alpha_i) \quad n:\text{even} \quad (5a)$$

$$a(t)=1+A'e^{-\sigma_0 t}+\sum_{i=1}^{(n-1)/2}A'_i e^{-\frac{a_i}{2}t}\cos(\omega_i t+\alpha'_i) \quad n:\text{odd} \quad (5b)$$

where $\omega_i=\sqrt{b_i-(\frac{1}{2}a_i)^2}$

The following are observed:

1. Even functions exhibit non-zero values (which decrease with ω_s) at t=0. Their overshoots are higher than those of odd function.
2. As ω_s increases, delay time becomes longer.
3. As A_p increases, overshoot becomes higher and the delay time longer.

Unit step responses are shown in Fig. 8 ω_s = 1.1, 2.0 and A_p=1.0. Cases A, B, and C are plotted in Fig. 9. Case A and Case B are almost identical.

V. Impulse Responses

The impulse responses are obtained by applying the inverse Laplace transformation on H(s) of equation (1).

$$h(t)=B_0(t)+\sum_{i=1}^{n/2}B_i e^{-\frac{a_i}{2}t}\cos(\omega_i t+\beta_i) \quad n:\text{even} \quad (6a)$$

$$h(t)=B'_0 e^{-\sigma_0 t}+\sum_{i=1}^{(n-1)/2}B'_i e^{-\frac{a_i}{2}t}\cos(\omega_i t+\beta'_i) \quad n:\text{odd} \quad (6b)$$

Characteristics similar to step responses have been observed in the impulse responses. It is

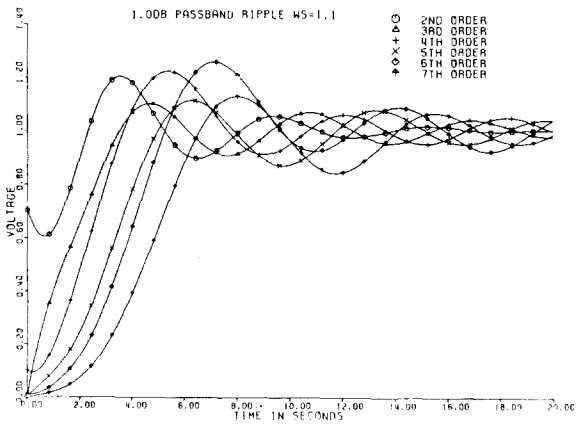

(a)

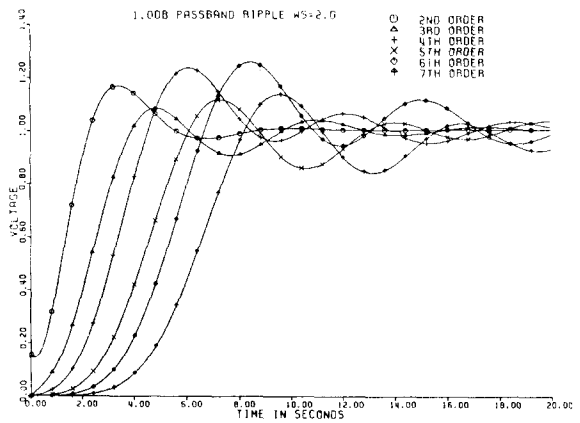

(b)

Fig. 8. Unit step response for Ap = 1.0 : (a) ω_s = 1.1, (b) ω_s = 2.0.

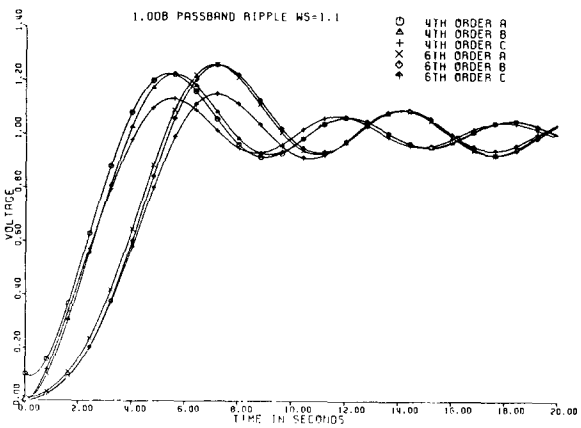

(a)

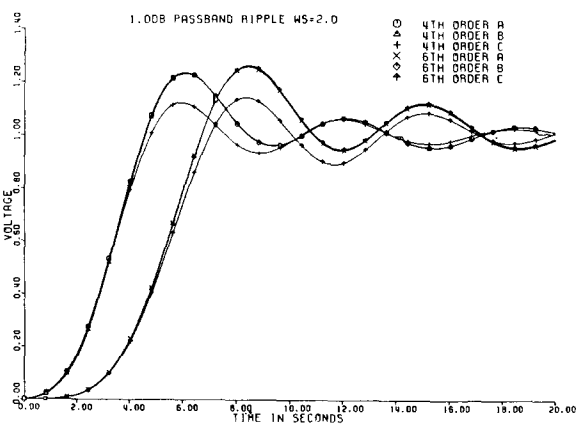

(b)

Fig. 9. Unit step responses of Cases A, B, C : (a) ω_s = 1.1, (b) ω_s = 2.0.

worth noting that the impulse exists in h(t) when n is even. And for odd n the σ_0 becomes smaller for increasing ω_s. Impulse responses are shown in Fig. 10 for ω_s=1.1, 2.0 and A_p= 1.0. Cases A, B, and Care compared in Fig. 11.

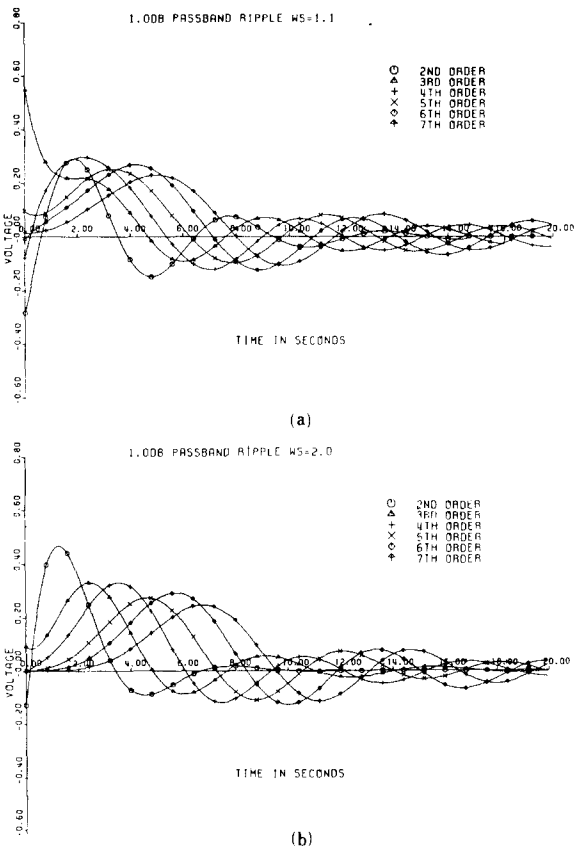

Fig. 10. Impulse response for Ap = 1.0 : (a) ω_s = 1.1, (b) ω_s = 2.0.

VI. Conclusions

The phase and group-delay have been examined. The time domain characteristics of the elliptic filters have been analyzed and compiled for various stopband frequencies and passband ripples. Case A, B, and C have also been compared for n=4 and n=6. All figures have been plotted by a VERSATEC D1200A plotter using an AMDAHL 5850 computer.

References

[1] D.E. Johnson, *Introduction to Filter Theory.* Englewood Cliff NJ: Prentice-Hall, 1976.

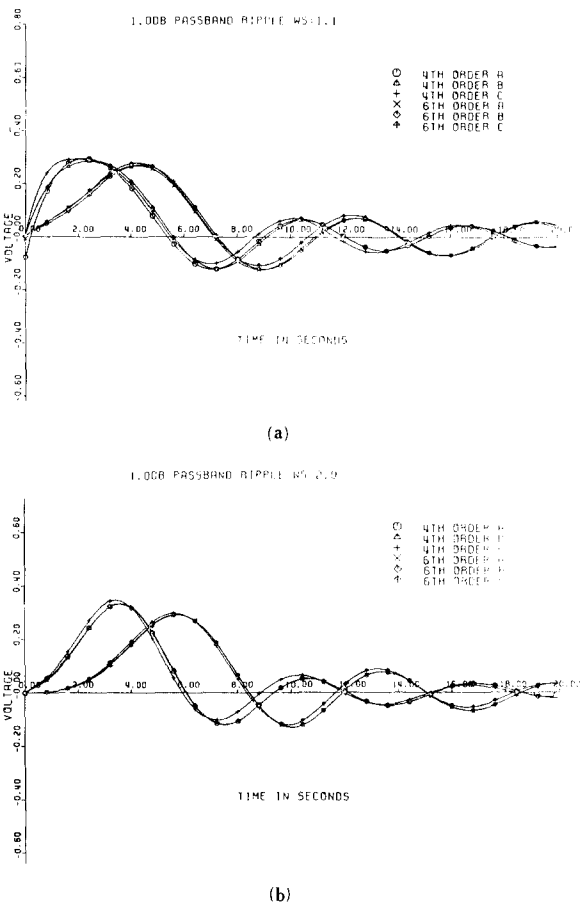

Fig. 11. Impulse response comparison of Cases A, B, C : (a) ω_s = 1.1, (b) ω_s = 2.0.

[2] L.P. Huelsman and P.E. Allen, *Theory and Design of Active Filters.* New York: Mcgraw-Hill, 1980.

[3] H.P. Moore, D.E. John son, and J.R. Johnson, "An active circuit for elliptic-type filters," *IEEE Trans. Circuits and Syst.*, vol. CAS-27, pp. 328-331, Apr. 1980.

[4] D.Y. Kim, "A new approach in the synthesis and analysis of elliptic filters," *Ph.D. thesis, Univ. of Manitoba,* Canada, 1984.

[5] A.B. Williams, *Electronic Filter Design Handbook.* New York: Mcgraw-Hill, 1981.

[6] R. Saal, *Handbook of Filter Design.* Berlin: AEG-Telefunken, 1979.

[7] D.Y. Kim and H.K. Kim, "Some results in elliptic filter characteristics," *IEEE Circuits and Systems Magazine,* in print for publication in 1985. *